

Journal of Biological Sciences

ISSN 1727-3048

science
alert

ANSI*net*
an open access publisher
<http://ansinet.com>



Research Article

Structure and Molecular Dynamic Regulation of FKBP35 from *Plasmodium knowlesi* by Structural Homology Modeling and Electron Microscopy

¹Jovi Silvester, ¹Herman Umbau Anak Lindang, ²Lee Ping Chin, ¹Lau Tiek Ying and ¹Cahyo Budiman

¹Biotechnology Research Institute, Universiti Malaysia Sabah, JI UMS, 88400 Kota Kinabalu Sabah, Malaysia

²Faculty of Science and Natural Resources, Universiti Malaysia Sabah, JI UMS, 88400 Kota Kinabalu Sabah, Malaysia

Abstract

Background and Objective: The 35 kDa FK506-binding proteins (FKBP35) of plasmodium parasite is a member of peptidyl prolyl *cis-trans* isomerase consisting of FK506-binding domain (FKBD) and tetratricopeptide repeat domain (TPRD). A comprehensive understanding of structure and function relationship of this protein is needed as a platform for development of novel antimalarial drugs with no resistance effect. However, structural study of full-length FKBP35 is hampered by some issues on molecular size and dynamic due to its structural flexibility. Therefore, this study aimed to analyze full-length structure of FKBP35 from *Plasmodium knowlesi* (Pk FKBP35) and determine its dynamics using structural homology modeling and a transmission electron microscope (TEM). **Methodology:** Structural homology modeling was constructed using SWISS-MODEL and further validated using RAMPAGE, Global model quality estimation (GMQE), QMEAN statistical parameters and VERIFY3D. For electron microscopy analysis, purified Pk FKBP35 was placed on EM grid, negatively stained using 2% uranyl acetate and recorded under TEM. The image was then processed using ImageJ to classify the molecular shape of Pk FKBP35 based on circularity index. Flexibility analysis was conducted under PredyFlexy web server. **Result:** The 3D model of Pk FKBP35 was successfully built based on the template of 1p5q. The structure consists of 6 β -sheet and 10 α -helix secondary structures that dominates FKBD and TPRD, respectively, with high similarity to the domains of its homologous from *P. falciparum* and *P. vivax*. Negatively stained electron micrograph showed that Pk FKBP35 assumes in three conformations of elongated, hook and circular shapes, with preference conformation being circular shapes (72%). Meanwhile, flexibility prediction demonstrated that FKBD region is more flexible than TPRD. **Conclusion:** Three conformations concluded that Pk FKBP35 is a dynamic protein due to its flexibility properties. This dynamic might be important for acquiring the substrates. FKBD was found to modulate the flexibility of Pk FKBP35, probably due to the functional role of this catalytic domain and structurally dominated by β -sheet structure, which is more flexible than α -helix structure. Further, 3D model of Pk FKBP35 also suggested that the linker between the domains might involve in the structural dynamic.

Key words: FKBP, *Plasmodium knowlesi*, negative staining, structural homology modeling, malaria, peptidyl prolyl *cis-trans* isomerase

Citation: Jovi Silvester, Herman Umbau Anak Lindang, Lee Ping Chin, Lau Tiek Ying and Cahyo Budiman, 2017. Structure and molecular dynamic regulation of FKBP35 from *Plasmodium knowlesi* by structural homology modeling and electron microscopy. J. Biol. Sci., 17: 369-380.

Corresponding Author: Cahyo Budiman, Biotechnology Research Institute, Universiti Malaysia Sabah, JI UMS, 88400 Kota Kinabalu Sabah, Malaysia
Tel: +6088-320000

Copyright: © 2017 Jovi Silvester *et al.* This is an open access article distributed under the terms of the creative commons attribution License, which permits unrestricted use, distribution and reproduction in any medium, provided the original author and source are credited.

Competing Interest: The authors have declared that no competing interest exists.

Data Availability: All relevant data are within the paper and its supporting information files.

INTRODUCTION

Malaria is a global health issue affecting almost half of the world population. This disease is caused by Plasmodium parasites, transmitted by infected female Anopheles mosquitoes¹. While antimalarial drugs are available in the market, recently concerns arose about the antimalarial drugs resistance in Plasmodium parasites. World Health Organization (WHO) had reported that out of 5 Plasmodium species that affect human, three of the Plasmodium parasites are known to have antimalarial drugs resistance². Therefore, to address this problem, alternative antimalarial drugs must be developed³⁻⁷.

A 35 kDa FK506-binding protein (FKBP35) was thought to be an appropriate target for development of antimalarial drug without resistance effect. This protein, as named, binds to and inhibited by an immunosuppressant drug FK506 or tacrolimus. Despite, FK506 has demonstrated to exhibit antimalarial effect⁸, the drug is not feasible to be used for long-term due to its drawback in suppressing the immune system. In attempts to replace FK506, further structural and functional studies on Plasmodium FKBP35 should be undertaken to discover more potential hotspots for novel antimalarial drugs.

FKBP35 is a member of peptidyl prolyl *cis-trans* isomerase (PPIase), a group of enzyme capable of catalyzing slow isomerization of *cis* prolyl bond during protein folding⁹⁻¹⁰. Previous studies on FKBP35 from *P. falciparum* (Pf FKBP35) and *P. vivax* (Pv FKBP35) revealed that this protein consists of two domains, N-terminal domain which has high similarity with human FKBP12 (designated as FKBP domain, FKBD) and C-terminal domain with tetratricopeptide repeat motif containing calmodulin binding signature (designated as tetratricopeptide repeat domain, TPRD)¹¹⁻¹³. This protein has been reported to bind FK506, to exhibit PPIase activity toward tetrapeptide substrate and chaperone function as well as inhibit calcineurin's phosphatase activity with and without FK506¹²⁻¹³.

This protein was believed to be expressed in all Plasmodium strains, including *P. knowlesi*, a simian malaria parasite that resides mainly among long-tailed macaques (*Macaca fascicularis*) and pig-tailed macaques (*M. nemestrina*) which are commonly found in Southeast Asia¹⁴⁻¹⁶. Naturally acquired human infections with *Plasmodium knowlesi* are endemic to Southeast Asia with the highest prevalence being in Malaysian Borneo¹⁷. Referring to the idea of FKBP35 from *P. falciparum* and *P. vivax*, study on FKBP35 from *P. knowlesi* (designated as Pk FKBP35, hereafter), might provide the platform for developing an antimalarial drug specifically targeting *P. knowlesi*.

While functional studies have been extensively done, structural studies on this protein remain to be limited. Atomic structures of FKBD and TPRD of FKBP35 are available, however there has not been any structural analysis on the full length of FKBP35. FKBD of Pf and Pv FKBP35 showed significant similarity to human FKBP12 and underwent structural changes upon binding to FK506^{4,11,18-19}. The structures of FKBD also revealed unique active site configuration at this protein as compared to human FKBP12, in which His87 and Ile90 of human FKBP12 were replaced by Cys and Ser, respectively, at Plasmodium FKBD. Meanwhile, TPRD folds into a canonical structure of TPR consisting of three repeating motifs, each comprising two helices plus an additional α -helix¹⁸.

This protein was found to be in dimeric form in solution with the size of about 75 kDa¹³, which is still in the range for crystallography work, yet too big for NMR spectroscopy. However, the absence of a crystal structure on the full-length FKBP35 might suggest that there are some issues on crystallizability of this protein. We speculated that flexibility of this protein promotes unsuccessful attempts on crystallization of the full length structure of FKBP35. Sousa²⁰, proposed that structural flexibility is a source of dynamic structural heterogeneity which presents an entropic barrier to crystallization.

To address this obstacle, structural homology modeling and single particle electron microscopy (EM) are promising tools to enable the visualization of the full-length structure of FKBP35. Structural homology modeling refers to the process of building a model from such a structural template²¹. With the availability of experimental atomic structures in Protein Data Bank (PDB) supported with advance computation technology, structural homology modeling has become a popular tool to access theoretical three-dimensional (3D) structures of molecular targets for the last decades²². In addition, single particle EM is considered as an emerging and versatile tool in structural biology²³. This technique employs a negative staining or frozen hydration treatment on the sample with no requirement on crystallization and constrain on flexibility. Indeed, EM has been proven to be successful in studying 2D or 3D structures of proteins and macromolecular complexes²⁴⁻²⁶. Despite the structural determination being limited by low resolution models, recent development on EM, however, was able to reach near atomic resolution²⁴⁻²⁵. Compared to frozen hydration technique followed by observation under cryo-EM, negative staining is a considerably simple treatment to visualize biological molecules under EM in which the samples are embedded in a thin layer of dried heavy metal salt to increase specimen contrast²⁶⁻²⁷. The

negative stain technique allows us to observe smaller molecules due to the high contrast²⁸⁻²⁹. This technique is usually combined with 2D image classification of molecules to enable observation of the heterogeneous molecule population dynamics which might arise from flexible protein²⁸.

In this study, three dimensional (3D) model was built displaying two canonical structures belong to FKBD and TPRD. The negatively stained Pk FKBP35 molecules were visualized under transmission electron microscope (TEM). A 2D image classification of the molecules revealed that this protein is highly dynamic with three possible conformation: Elongated, hook-shape and circular. *In silico* analysis revealed that the flexible residues are mostly localized in FKBD. Following that, the relationship of the structural dynamic of Pk FKBP35 with its function was discussed.

MATERIALS AND METHODS

Chemicals: All chemicals were purchased from Nacalai Tesque, Inc. (Kyoto, Japan) and used without further purification except when mentioned specifically. The experiment was performed at Biotechnology Research Institute, Universiti Malaysia Sabah in accordance with the institute guidelines and regulations from July 2016-June 2017.

Protein: The protein used in this study was purified recombinant full-length of Pk FKBP35. The protein was dissolved in 20 mM phosphate buffer pH 8.0 buffer with the final concentration of 0.1 mg mL⁻¹. Prior to the analysis, purity of the protein was checked using 15% gel of SDS-PAGE. To remove aggregated proteins and other particles, the sample was centrifuges at 30,000 g for 30 min at 4°C followed by filtration of the supernatant using 0.22 µm filters (Millipore Corp., Bedford, MA).

Structural homology modeling and validation: The amino acid sequence of Pk FKBP35 was retrieved from PlasmoDB (Gene ID: PKNH_1467100) and used as targets for homology modelling using the SWISS-MODEL server³⁰⁻³². The latter performed the target template sequence alignment after searching the putative X-ray template proteins in PDB for generating the 3D models for all target sequences. The best homology models were validated according to Global model quality estimation (GMQE) and QMEAN statistical parameters^{33,34}. Stereo chemical quality of the model was evaluated using Ramachandran plot³⁵ and VERIFY3D³⁶.

Electron microscopy: Conventional negative staining procedure was used to prepare the EM specimen as described

Ohi *et al.*²⁸, with some modifications on sample amount and concentration of uranyl acetate. In this study, we used lower amount of sample volume to avoid aggregation and clarity during observation. However, we used higher concentration of uranyl acetate to increase the contrast. Briefly, a 10 µL of sample solution was adsorbed to a carbon film on 200 mesh gold grid (Quantifoil) washed with two drops of deionized water and stained with two drops of freshly prepared 2% uranyl acetate for 5-10 min.

Specimen was then imaged at room temperature using a Tecnai G2 Spirit BioTwin transmission electron microscope (FEI) operated at an acceleration voltage of 120 kV. Images were taken at various magnification and a defocus (from 500-50 nm) using low-dose procedures. The image captured was saved for further analysis.

Image processing: The images captured in the TEM was then processed and analyzed utilizing the ImageJ software, adopting the method described by Papadopoulos *et al.*³⁷ for protein counting and averaging. Briefly, the image format was changed to 8-bit format and the measurement scale was set. After that, the region of interest was chosen and the threshold image of the particles was obtained from the threshold command. The threshold image obtained was then used to assist the software to automatically count the protein particles according to the parameter, which is the surface area between 10-15 nm², set in the software. The data obtained from the ImageJ software analysis was further analyzed using a micrograph data analysis. The circularity of the molecules were categorized based on its circularity index³⁸. A circularity index of 1.0 indicates a perfect circle. As the value approaches 0, it indicates an increasingly elongated polygon.

Flexibility analysis: The Pk FKBP35 protein flexibility was predicted using PredyFlexy web server. The Pk FKBP35 amino acids sequence was derived from the gene sequence of FKBP35 that was used in the software. The PredyFlexy server just needs the amino acid sequence of the protein to predict the flexibility of the proteins needed. Besides predicting the protein flexibility, this server can also be used to predict local structure. The prediction was done using classical normalized B-factors (B-factor Norm) and normalized RMSF (RMSF Norm) from molecular dynamics. There were a few categories used to classify the protein flexibility, which includes rigid, intermediates and flexible³⁹. The software algorithm classifies every input residue as rigid, intermediate or flexible and also outputs putative normalized B-factors and root mean square fluctuations, from molecular dynamic simulations⁴⁰.

RESULTS

Protein: Pk FKBP35 used in this study was obtained from heterologous expression system under *Escherichia coli* BL21 (DE3) system. The purity of the protein was considerably high (Fig. 1) hence, acceptable for the EM analysis. Apparent size of this protein was about 35 kDa in 15% SDS-PAGE, which was comparable to the size of Pf FKBP35. In solution, due to its high similarity with Pf FKBP35, we believe that Pk FKBP35 also assumed in dimeric form with the size of 70-75 kDa.

Three-dimensional (3D) model of Pk FKBP35: Structural homology modeling was constructed using SWISS-MODEL platform to obtain a 3D model of full length Pk FKBP35. Crystal structure of FKBP51 (PDB ID 1P5Q) was selected as a template for the model construction. The template displayed 31.29% similarity to Pk FKBP35 in its amino acid sequences. The model revealed Pk FKBP35 (Fig. 2a) folds into two canonical structures from its N-terminal, FKBP and TPRD, which corresponded to Pk FKBD and Pk TPRD, respectively. The schematic diagram of the domains organization is shown in Fig. 2b. In overall, Pk FKBP35 is dominated by helical structures (10, helix A-J), which more than 70% of helices (helix D-K) were spatially located at TPRD. The helical structures in Pk FKBD (helix A: Lys96-Ser103 and helix B: Ser117-Tyr119) were relatively shorter than that of located at Pk TPRD. The helices in Pk TPRD composed by Asn157-Lys177 (helix C), Ile180-Phe193 (helix D), Asp203-Asn227 (helix E), Phe229-Ile242 (helix F), Val247-Phe260 (helix G), Leu263-Leu276 (helix H), Val281-Asp310 (Helix I) and Gly312-Ser321 (Helix J). In addition, Pk FKBP35 consists of 6 β -sheets which all of them are located at FKBD. These β -sheets are built up by Val38-Arg43 (β 1), Gly57-Lys68 (β 2), Lys73-Asp76 (β 3), Pro84-Leu89 (β 4), Asn108-Leu115 (β 5) and Leu136-Arg146 (β 6). In overall, the model displayed R.M.S.D of 0.52 Å with 1P5Q for about 259 atoms.

Validation of 3D model of Pk FKBP35 was performed using several approaches to ensure that the build model is chemically, physically and statistically acceptable. First validation through Ramachandran plot (Fig. 3) revealed that most of residues are located in acceptable regions (favorable or allowed). However, 5 residues (1.5%) are found to be in outlier region. In the model, most of these residues (Glu48, Ser78, Lys149 and Thr156) are located at flexible loop structure. At this position, steric coordinate of these residues are statistically difficult to be predicted, thus it is practically acceptable for the residues located at the flexible structure to be in outlier region under Ramachandran map. Another residue located at outlier region is Pro84, which is located at

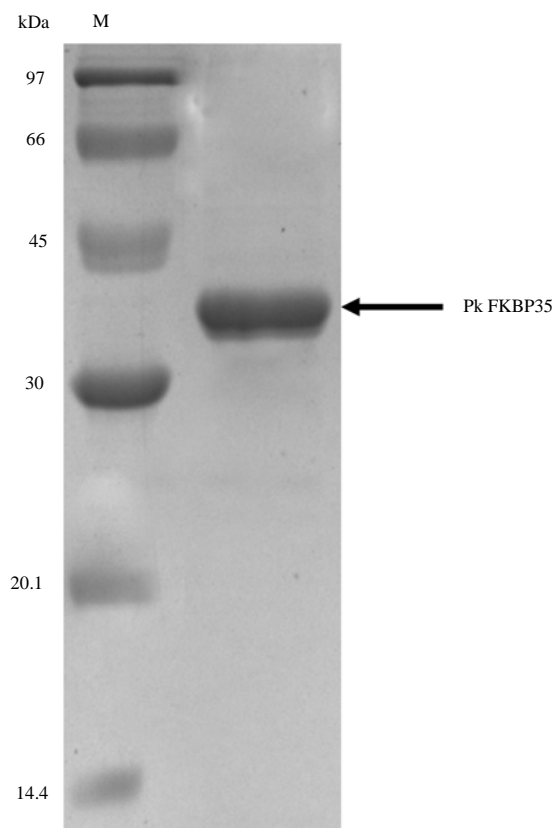


Fig. 1: Purity of Pk FKBP35 as visualized under 15% SDS-PAGE
M line corresponds to low molecular weight protein markers. Band corresponds to Pk FKBP35 is indicated by arrow

the N-terminus of β 4. Proline, in addition to Gly, is one of residue that often found to be in outlier region under Ramachandran map. In case of proline, cyclic side chain of proline restricted the rotation around the bond and hence it is acceptable to be often found in outlier region. Accordingly, validation using Ramachandran plot indicated that the model is acceptable.

Further, Global model quality estimation (GMQE) structural validation showed that the model has GMQE score of 0.61 out of 0-1 scales. This indicated that quality of the model is moderate. GMQE is calculated based on the combination of properties from the target-template alignment, which indicated accuracy of the model build with the alignment and template. Moderate score of the model of Pk FKBP35 might be due to the absence of structural template with high similarity to Pk FKBP35.

In addition, QMEAN Z-score of the model of Pk FKBP35 was found to be -2.65. The score reflects absolute quality of global and local based on a one single model and indicates the quality of the model as compared to the experimental

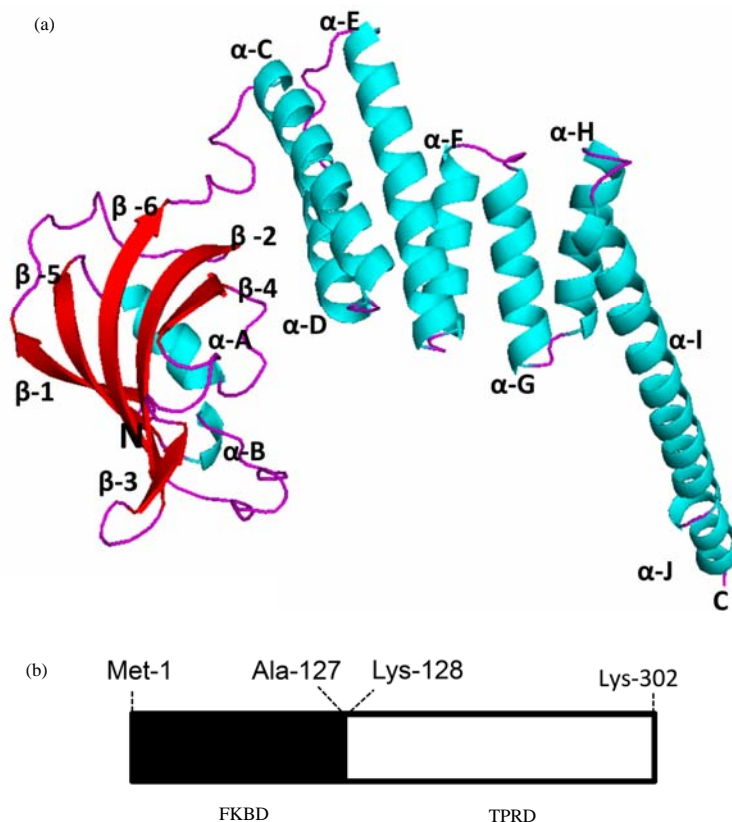


Fig.2(a-b): Full-length structure of Pk FKBP35 displayed as (a) Cartoon model of its three-dimensional (3D) model and (b) Schematic diagram of its primary structure showing the domains organization

structures. The minimum score for the model to be considered as a good quality of structural model is -4.00. Accordingly, the model of Pk-FKBP35 was considered as a good model as its Z-score is higher than -4.00.

Lastly, the compatibility of an atomic model (3D) with its amino acid sequence (1D) was validated under Verify3D. Verify3D verifies if the protein model is correct or no through assignment of structural class based on its location and environment. Verify3D analysis of the model of Pk FKBP35 revealed that 66.09% of the residues had an averaged 3D-1D score more than 0.2. The required minimum score of the residues is higher than 0.2 is 65%. This indicated that this value is quite close to the minimum standard, however it suggests that the model structure of Pk FKBP35 is good enough.

Microscope: The observation was performed on 9 grids. The typical micrograph of Pk FKBP35 reflected in 2D is shown in Fig. 4. As negative staining resulted in the target molecules to be brighter than the background, we believe that Pk FKBP35 molecules are bright objects under the scope. Aggregation of molecules was on some grids and distinguishable to properly

folded proteins in their contrast. Aggregated proteins appeared as extremely dark objects due to accumulation of proteins that formed a thick specimen. A single molecule is relatively thin enough for electron transmission so that the contrast is not as dark as aggregated proteins. Accordingly, the target molecules for further analysis in this study were separated from the target area. In total, 637 molecules were identified and targeted for further analysis.

Image analysis-based 2D surface area of the target molecules was then performed using the ImageJ software. Average surface area of the molecules was about 15 nm², which corresponds to the accumulation of 2D structural sizes of FKBD and TPRD of *P. falciparum*. Interestingly, all molecules in 9 grids have almost similar surface area size (Fig. 5) indicating that the sample is homogenous.

Further observation on the shape of the molecules, however, revealed shape differences of the molecules in all grids. All molecules with the index between 0.24-0.75 were assumed in the hook shape, an intermediate shape of elongated and perfect circle. The result showed that the molecules exhibited three forms of 2D shapes: Elongated,

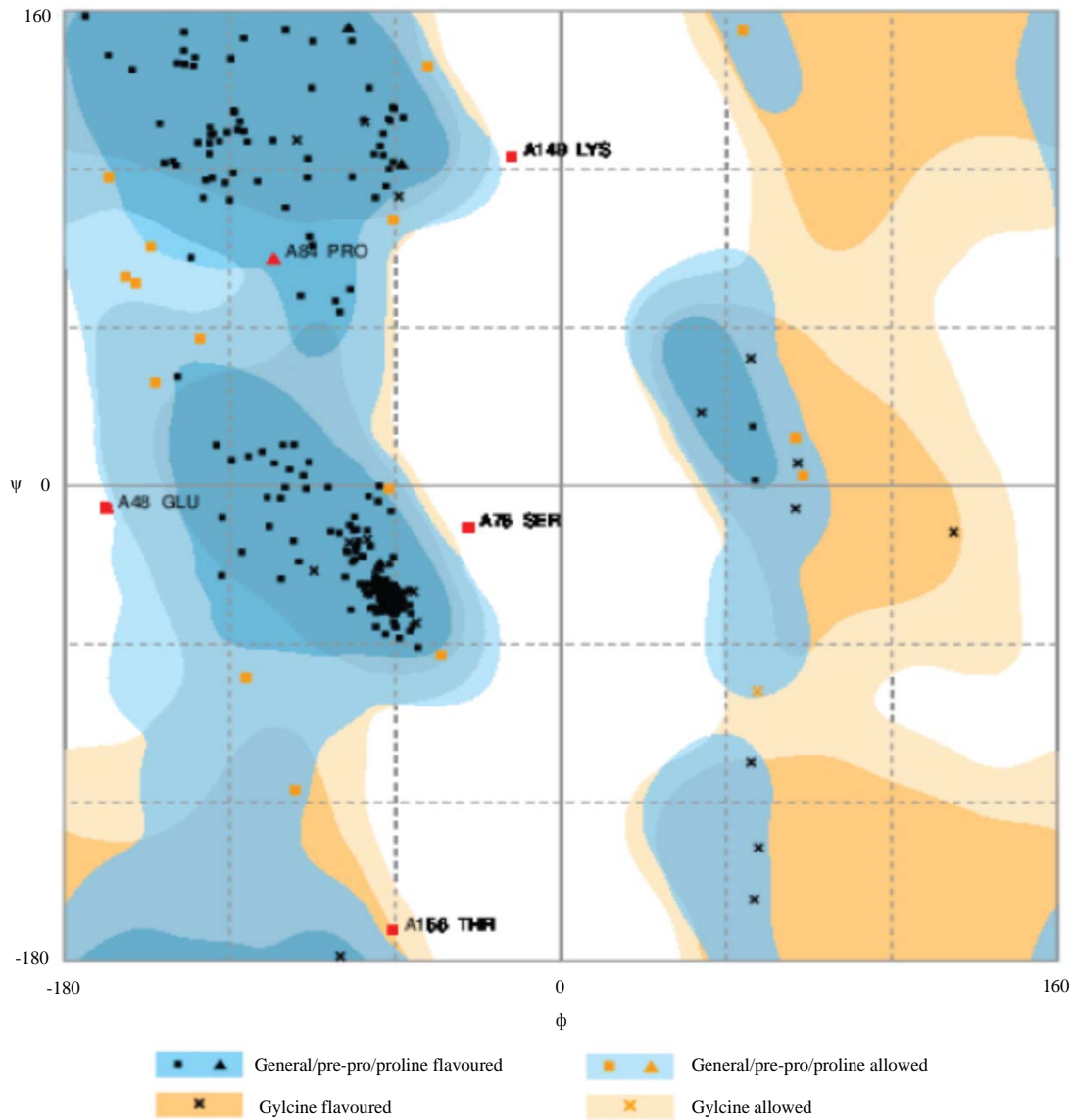


Fig. 3: Ramachandran plot of three-dimensional (3D) model of Pk FKBP35

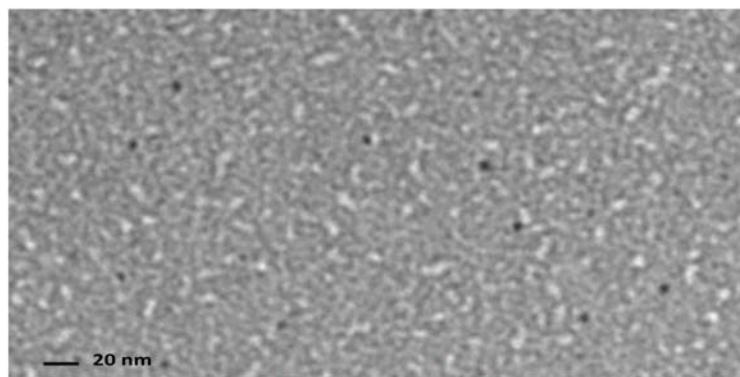


Fig. 4: Micrographic representatives of uranyl acetate negatively-stained Pk FKBP35 under transmission electron microscope (TEM)

hooked and circular (Fig. 6). However, circular shapes were more dominant (72%), followed by hooked shape (27%) and the remaining molecules were in elongated shapes. The representative molecules exhibiting circle, hooked and elongated shapes are shown in Fig. 7.

Flexibility analysis: The result shown in Fig. 8 revealed that flexible residues mostly located in the region of FKBD (Met1-Ala148). Some short fragments, however, in this region showed extremely low flexibility index, particularly in Ser113-Gln120 and Asp145-Gln148. Meanwhile, residues located at TPRD (Lys149-Lys323) are less flexible. This result indicated that, on the overall, FKBD is structurally more flexible than TPRD. This flexibility was speculated to play an important role in conformational changes of Pk FKBP35.

Proposed structural dynamic: Relationship among three shapes of Pk FKBP35 is shown in Fig. 9 revealing the conformational changes of Pk FKBP35 to undergo, in sequential orders, from elongated to hook and then circular shapes. This indicated that Pk FKBP35 was not structurally static, rather it is dynamic in which elongated shape was convertible to hook and further to circular shapes. The conversion is reversible, in which circular shape would able to change to elongated shape through hook shape. Since circular shape is more dominant, as shown in Fig. 6, direction of structural changes of Pk FKBP35 is more to circular shape.

DISCUSSION

Some of the key challenges in protein structural studies are associated with two inherent properties of the proteins: (i) size and (ii) flexibility. NMR spectroscopy allows us to capture the dynamics of flexible protein in solution. However, the technique is only preferable for small size proteins⁴¹⁻⁴². In overcoming this issue, X-ray crystallography technique could

potentially work well for proteins with higher size⁴³, although this technique requires a crystallization step which could not be applied to all proteins⁴⁴. The main issue in protein

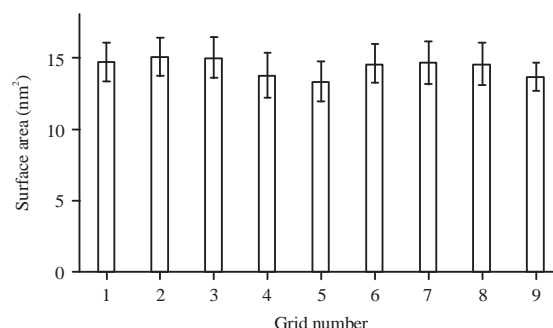


Fig. 5: Average of surface area of Pk FKBP35 molecules observed on several grids

Bars represent standard of deviation of the mean

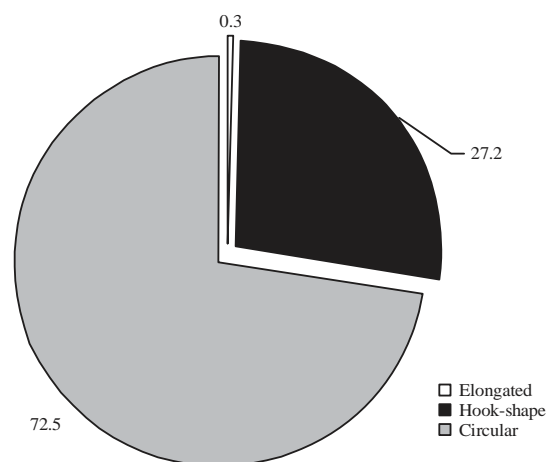


Fig. 6: Distribution of molecular shapes of Pk FKBP35

The number represents the percentage (%) of molecules observed in each respected shapes. The shapes were classified based on its circularity index: Elongated (<0.249), hook (0.25-0.749) and circular (>0.75)

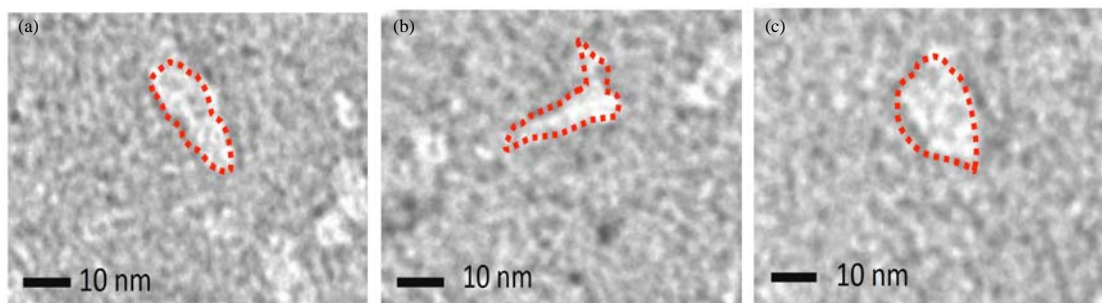


Fig. 7(a-c): Representatives of (a) Elongated, (b) Hook and (c) Circular shapes of Pk FKBP35 under transmission electron microscope (TEM)

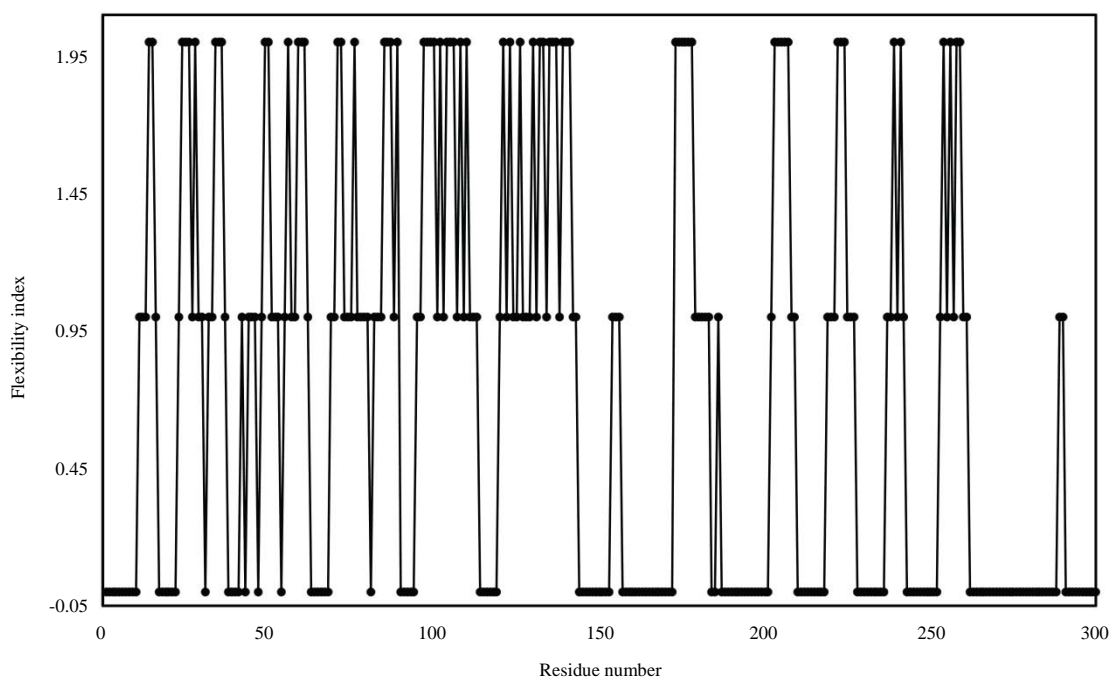


Fig. 8: Predicted flexibility score of the residues of Pk FKBP35 as predicted using PredyFlexy

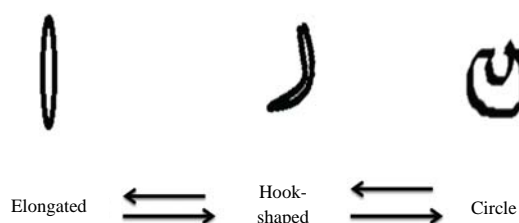


Fig. 9: Possible relationships among the molecular shapes of Pk FKBP35 that reflects its structural dynamic

crystallization is flexibility, where highly flexible proteins are not easy to be crystallized due to in homogeneous conformation of the proteins^{43,45}. Besides, size of the protein also limits this technique, in which the proteins with extremely large size are not relatively easy to be crystallized^{43,46}. In particular, the proteins with quaternary structure due to complex formation with other proteins, X-ray crystallography has serious problem in solving the structure. Structural homology modeling and EM are alternative techniques to address the problems that are unable to be solved either by NMR spectroscopy or X-ray crystallography^{44,47}. Structural homology modeling overcomes the issues on determination of protein structure by means of experimental methods such as X-ray crystallography or NMR spectroscopy, including time consuming and crystallizability of many proteins⁴⁸. The

limitation in structural homology modeling is the availability of structural template and computer algorithm reliability. Meanwhile, the only limitation on EM technique is resolution, which up to now is still beyond atomic scale. However, current progress in the field demonstrated tremendous improvement on the techniques in overcoming the aforementioned limitations. In respect to number of template, the number of atomic structures deposited in Protein Data Bank (PDB) is exponentially increased every year, which may serves as structural templates for the modeling⁴⁹. Further, some cryo-EM experiments on reconstruction of 3D models of some proteins have also succeeded to undergo to near atomic resolution⁵⁰.

Full-length FKBP35 was actually moderate in size (35 kDa in monomer or 70 kDa in dimer¹³) for crystallization, yet definitely is too big for NMR spectroscopy. However, there has not been any successful attempt reported for crystal structure of full-length FKBP35. The only available atomic structure was its isolated domains, either FKBD or TPRD^{4,11,18-19}. It was assumed that flexibility issue is the main concern on the failure of crystallization of full-length FKBP35. Given that FKBP35 had exhibited a dual function that was independently regulated by different domains¹², full-length structure of FKBP35 might provide some hints on structural regulation of the dual function of FKBP35.

The 3D model of Pk FKBP35 constructed in this study was considerably an acceptable model based on the structural validation as explained before. In fact, the quality of the 3D model could be much better for the isolated domain. Detail analysis on verify3D indicated that the residues that having issues in the structural validations were located at the linker between FKBD and TPRD, in addition to N- and C terminal residues which were known to be flexible. This indicated that the validity of atomic coordinates in the 3D model of the domains have no issues. This might also explain the unsuccessful attempts on crystallization of full-length FKBP35 is likely due to flexibility of the domain linker. In addition, the template (1P5Q) used for the modeling was not considerably low similarity with Pk FKBP35. This might account for moderate score of structural validation of Pk FKBP35 under some platforms. Nevertheless, 1P5Q was the only available structure of PPIase member containing TPR domain, hence was selected as a template. Pk FKBP35 was rather similar to FKBP35 from *P. falciparum* and *P. vivax* with amino acid sequence similarities are about 80%. However, none of full length atomic structures were reported for FKBP35 from *P. falciparum* or *P. vivax*. The only atomic structures available are isolated FKBD and TPRD from those proteins.

Nevertheless, structural features catalytic domain of Pk FKBP35 are in good agreement with atomic structure of FKBD from *P. falciparum* and *P. vivax* demonstrating the dominance of β -sheets structure^{4,11,19}. In fact, canonical FKBP structures from various organisms were reported to be dominated with β -sheets structure. Structural alignment of Pk FKBD with FKBD from *P. falciparum* and *P. vivax* showed high structural similarity with R.M.S.D of 2.34 and 1.27 Å, respectively. High structural similarity was also obtained when 3D model Pk FKBD was aligned with human FKBP35 (R.M.S.D of 1.75 Å). Meanwhile, TPR motif is indeed dominated by helical structures. Only a single structure of TPRD from *P. falciparum* was successfully crystallized so far¹⁸. Pk TPRD and TPRD from *P. falciparum* showed high similarity with R.M.S.D of 0.51 Å.

The use of negatively stained EM technique rather than cryo-EM was considered due to the simplicity and cost efficiency of the technique. However it is noteworthy to understand that the use of EM for FKBP35 is actually tricky due to the size of this protein. While size of this protein is in the range for X-ray crystallography, the size was considerably small for EM technique. Accordingly, this study not only attempted to provide a 2D structure and structural classification of FKBP35 but also determine the feasibility of structural studies of FKBP35 using EM.

The result confirmed that Pk FKBP35 could be observed under EM with negative staining treatment. It was believed that the use of negative staining is important for relatively small size proteins due to its low contrast feature. The success of observing this protein under EM suggests that FKBP35 from other Plasmodium are also feasible to be observed. Noteworthy, there is possibility of the molecules observed under microscope are also mixture of FKBP35 and contaminants. However, we believed that contaminant proteins are really in minimal amount since purification step yielded a single band in SDS-PAGE (Fig. 1). The fact that selected molecules for analysis having similar surface area size (Fig. 5) also support that the molecules used in this study is in high purity. Meanwhile, we also believed that the analyzed molecules were not aggregated proteins due to relatively low contrast as compared to aggregated proteins.

Further analysis on 2D shape of Pk FKBP35 revealed the first evidence of three conformational changes of this protein: elongated, hook-shaped and circular. These conformations suggest that Pk FKBP35 is flexible which can undergo structural changes that regulated by the movement of the domains. In elongated structure, FKBD and TPRD were separated at their highest distance. There is non-covalent interaction between these two domains at this conformation. Movement one or two domains leads to the conformational changes to be a hook-shaped or further completely in a circular shape. In circular shapes the distance between two domains was at their closest distance and could possibly have a non-covalent interactions. Meanwhile, in a hook-shape, the distance of two domains is relatively closer than that of in elongated shape, yet further than that of circular shape. However, the technique used in this study did not allow localization of the domains due to its low resolution.

In addition, conformational changes of Pk FKBP35 are assumed to be associated with its function. In respect to a dual function of FKBP35, this protein recognizes two types of substrates which differ in sizes: Short peptide and protein^{12,13}. Small substrate (short peptide) does not require wide region of FKBP35 to interact, while wider surface area of FKBP35 might be needed to properly bind to protein substrate. Elongated structure might be more appropriate for small substrate, however larger substrates would require wider interaction area, hook or circular shaped are considerably more capable of binding to protein. In these shapes, two domains are in close distance thus two domains might contribute to provide more interaction sites for larger substrate. Alternatively, in hooked or circular shapes, the larger

substrates can be possibly accommodated in the space between the two domains. This suggested that conformational changes of Pk FKBP35 might be due to the function of this protein in binding with the substrates. Based on this reason also, we proposed that the conformational changes as shown in Fig. 9 is reversible to allow the protein bind to a variety of substrate types. The reversibility was also in good agreement with structural flexibility issue. If the protein was in rigid structure, there will be no conformational changes and only one conformational state was observed under EM. The changes from elongated to circular structures, without hooked structure, were believed to be difficult due to the high-energy requirement. It would be interesting to note that hooked and circular shapes were more dominant as compared to elongated shapes. Thermodynamically, circular and hooked shapes have lower entropy than elongated structure. Accordingly, these two structures are energetically more favorable and stable. In addition, there was no report for ATPase activity of PPIase, including FKBP's family member. This indicated that structural flexibility of Pk FKBP35 is apparently under allosteric regulation with no external energy required.

The remaining question is dealing with which domain regulates conformational changes of Pk FKBP35. FKBD region is more flexible than TPRD as clearly indicated by Fig. 8. This result was intriguing, since Monaghan and Bell¹², reported that TPRD is the domain where protein substrate interacts with, the flexibility is supposedly located at this domain. Nevertheless, high flexibility of FKBD might be due to the function of this domain as a catalytic domain^{12,13} that was responsible for binding to small peptide substrate. High flexibility of this domain is important to allow the protein to capture substrate and exhibit an optimum catalytic efficiency. Budiman *et al.*⁵¹ reported that high flexibility of catalytic domain of FKBP22 from *Shewanella* sp. SIB1 promotes higher catalytic efficiency of this protein. In addition, given TPRD is in dimeric structure, the flexibility of this protein is probably restricted by the dimerization of the domain. The structural restriction by dimeric structure was also reported by Budiman *et al.*⁵² in FKBP22.

It is also interesting that 3D model of Pk FKBP35 showed that secondary structure of TPRD is mostly formed by helical structure, while FKBD is by beta sheet structure. The side chains of beta strands are arranged alternately on opposite sides of the strand. The distance between amino acids in a beta strand is 3.5Å which is longer than the 1.5Å distance in α strands. Due to this, β sheets are more flexible than α helices and can be flat and somewhat twisted⁵³⁻⁵⁴. Accordingly, it is

acceptable that TPRD is less flexible than FKBD due to the high content of helical structure. Furthermore, by taking into account the 3D Pk FKBP35, it is acceptable, yet arguable, to include the linker between Pk FKBP and Pk TPRD as a "structural neck or hinge" that involved in the movement of Pk FKBD and dynamic in overall structure of Pk FKBP35.

Altogether, this study demonstrated the feasibility of EM on structural analysis of FKBP35. High sequence similarity among FKBP35 from all Plasmodium parasites suggested that other FKBP35 exhibited conformational changes as been observed in Pk FKBP35. Further study on 3D structure of full-length Pk FKBP35 is feasible to be done using other techniques of EM, including single particle analysis or molecular electron tomography under cryo-EM.

CONCLUSION

Three-dimensional model of full length Pk FKBP35 revealed that the protein is arranged in two separated domains, Pk FKBD and Pk TPRD. The structure is apparently dynamic as shown under EM which demonstrated three structural conformations: Elongated, hook and circular shapes, with conformation preference of circular shapes. These three conformation suggested flexibility of this protein which was assumed to be important for acquiring the substrates. Furthermore, we found that this flexibility is mostly located at FKBD region, which probably plays an important role in facilitating this domain in capturing the substrate and maximizing the catalytic efficiency.

SIGNIFICANCE STATEMENTS

This study discovers the structural feature of full-length Pk FKBP35 and its dynamic that can be beneficial for development of antimalarial drug with no resistance effect. This study help the researcher to uncover the critical areas of structural flexibility of multi-domain proteins that many researchers were not able to explore. Thus, a new theory on structural dynamic regulation may be arrived at.

ACKNOWLEDGEMENTS

This work was supported by the Fundamental Research Grant Scheme (FRGS) funded by Ministry of Education, Malaysia under Grant No. FRG0395-ST-2/2014. The authors thank Carlmond Goh Kah Wun (Universiti Malaysia Sabah) for providing the purified FKBP35.

REFERENCES

1. Cox, F.E., 2010. History of the discovery of the malaria parasites and their vectors. *Parasites Vectors*, Vol. 3. 10.1186/1756-3305-3-5.
2. Cui, L., S. Mharakurwa, D. Ndiaye, P.K. Rathod and P.J. Rosenthal, 2015. Antimalarial drug resistance: Literature review and activities and findings of the ICEMR network. *Am. J. Trop. Med. Hyg.*, 93: 57-68.
3. Fidock, D.A., P.J. Rosenthal, S.L. Croft, R. Brun and S. Nwaka, 2004. Antimalarial drug discovery: Efficacy models for compound screening. *Nat. Rev. Drug Discov.*, 3: 509-520.
4. Kotaka, M., H. Ye, R. Alag, G. Hu and Z. Bozdech *et al.*, 2008. Crystal structure of the FK506 binding domain of *Plasmodium falciparum* FKBP35 in complex with FK506. *Biochemistry*, 47: 5951-5961.
5. White, N.J., 2004. Antimalarial drug resistance. *J. Clin. Invest.*, 113: 1084-1092.
6. Yeung, S., W. Pongtavornpinyo, I.M. Hastings, A.J. Mills and N.J. White, 2004. Antimalarial drug resistance, artemisinin-based combination therapy and the contribution of modeling to elucidating policy choices. *Am. J. Trop. Med. Hyg.*, 71: 179-186.
7. Wongsrichanalai, C., A.L. Pickard, W.H. Wernsdorfer and S.R. Meshnick, 2002. Epidemiology of drug-resistant malaria. *Lancet Infect. Dis.*, 2: 209-218.
8. Bell, A., B. Wernli and R.M. Franklin, 1994. Roles of peptidyl-prolyl *cis-trans* isomerase and calcineurin in the mechanisms of antimalarial action of cyclosporin A, FK506 and rapamycin. *Biochem. Pharmacol.*, 48: 495-503.
9. Lang, K., F.X. Schmid and G. Fischer, 1987. Catalysis of protein folding by prolyl isomerase. *Nature*, 329: 268-270.
10. Schmid, F.X., L.M. Mayr, M. Mucke and E.R. Schonbrunner, 1993. Prolyl isomerases: Role in protein folding. *Adv. Protein Chem.*, 44: 25-66.
11. Kang, C.B., H. Ye, H.R. Yoon and H.S. Yoon, 2008. Solution structure of FK506 Binding Domain (FKBD) of *Plasmodium falciparum* FK506 Binding Protein 35 (PffFKBP35). *Proteins: Struct. Funct. Bioinform.*, 70: 300-302.
12. Monaghan, P. and A. Bell, 2005. A *Plasmodium falciparum* FK506-Binding Protein (FKBP) with peptidyl-prolyl *cis-trans* isomerase and chaperone activities. *Mol. Biochem. Parasitol.*, 139: 185-195.
13. Yoon, H.R., C.B. Kang, J. Chia, K. Tang and H.S. Yoon, 2007. Expression, purification and molecular characterization of *Plasmodium falciparum* FK506-binding protein 35 (PffFKBP35). *Protein Expression Purif.*, 53: 179-185.
14. Singh, B. and C. Daneshvar, 2013. Human infections and detection of *Plasmodium knowlesi*. *Clin. Microbiol. Rev.*, 26: 165-184.
15. Coatney, G.R., W.E. Collins, M. Warren and P.G. Contacos, 1971. The primate malarias. U.S. National Institute of Allergy and Infectious Diseases, Washington, DC., USA., pp: 1-366.
16. William, T., J. Jelip, J. Menon, F. Anderios and R. Mohammad *et al.*, 2014. Changing epidemiology of malaria in Sabah, Malaysia: Increasing incidence of *Plasmodium knowlesi*. *Malar. J.*, Vol. 13. 10.1186/1475-2875-13-390.
17. Cox-Singh, J., T.M.E. Davis, K.S. Lee, S.S.G. Shamsul and A. Matusop *et al.*, 2008. *Plasmodium knowlesi* malaria in humans is widely distributed and potentially life threatening. *Clin. Infect. Dis.*, 46: 165-171.
18. Alag, R., N. Bharatham, A. Dong, T. Hills and A. Harikishore *et al.*, 2009. Crystallographic structure of the tetratricopeptide repeat domain of *Plasmodium falciparum* FKBP35 and its molecular interaction with Hsp90 C-terminal pentapeptide. *Protein Sci.*, 18: 2115-2124.
19. Alag, R., I.A. Qureshi, N. Bharatham, J. Shin, J. Lescar and H.S. Yoon, 2010. NMR and crystallographic structures of the FK506 binding domain of human malarial parasite *Plasmodium vivax* FKBP35. *Protein Sci.*, 19: 1577-1586.
20. Sousa, R., 1995. Use of glycerol, polyols and other protein structure stabilizing agents in protein crystallization. *Acta Crystallogr. D: Biol. Crystallogr.*, 51: 271-277.
21. Petrey, D. and B. Honig, 2005. Protein structure prediction: Inroads to biology. *Mol. Cell*, 20: 811-819.
22. Franca, T.C.C., 2015. Homology modeling: An important tool for the drug discovery. *J. Biomol. Struct. Dyn.*, 33: 1780-1793.
23. Cheng, Y. and T. Walz, 2009. The advent of near-atomic resolution in single-particle electron microscopy. *Annu. Rev. Biochem.*, 78: 723-742.
24. Grigorieff, N. and S.C. Harrison, 2011. Near-atomic resolution reconstructions of icosahedral viruses from electron cryo-microscopy. *Curr. Opin. Struct. Biol.*, 21: 265-273.
25. Zhou, Z.H., 2011. Atomic resolution cryo electron microscopy of macromolecular complexes. *Adv. Protein Chem. Struct. Biol.*, 82: 1-35.
26. Bartesaghi, A., A. Merk, S. Banerjee, D. Matthies, X. Wu, J.L. Milne and S. Subramaniam, 2015. 2.2 Å resolution cryo-EM structure of β -galactosidase in complex with a cell-permeant inhibitor. *Science*, 348: 1147-1151.
27. Adrian, M., J. Dubochet, J. Lepault and A.W. McDowell, 1984. Cryo-electron microscopy of viruses. *Nature*, 308: 32-36.
28. Ohi, M., Y. Li, Y. Cheng and T. Walz, 2004. Negative staining and image classification-powerful tools in modern electron microscopy. *Biol. Proced. Online*, 6: 23-34.
29. De Carlo, S. and J.R. Harris, 2011. Negative staining and cryo-negative staining of macromolecules and viruses for TEM. *Micron*, 42: 117-131.
30. McGuffin, L.J., K. Bryson and D.T. Jones, 2000. The PSIPRED protein structure prediction server. *Bioinformatics*, 16: 404-405.
31. Biasini, M., S. Bienert, A. Waterhouse, K. Arnold and G. Studer *et al.*, 2014. SWISS-MODEL: Modelling protein tertiary and quaternary structure using evolutionary information. *Nucl. Acids Res.*, 42: W252-W258.

32. Bordoli, L., F. Kiefer, K. Arnold, P. Benkert, J. Battey and T. Schwede, 2009. Protein structure homology modeling using SWISS-MODEL workspace. *Nat. Protoc.*, 4: 1-13.
33. Benkert, P., M. Kunzli and T. Schwede, 2009. QMEAN server for protein model quality estimation. *Nucl. Acids Res.*, 37: W510-W514.
34. Benkert, P., M. Biasini and T. Schwede, 2011. Toward the estimation of the absolute quality of individual protein structure models. *Bioinformatics*, 27: 343-350.
35. Lovell, S.C., I.W. Davis, W.B. Arendall, P.I. de Bakker and J.M. Word *et al.*, 2003. Structure validation by C α geometry: ϕ , ψ and C β deviation. *Proteins: Struct. Funct. Bioinform.*, 50: 437-450.
36. Eisenberg, D., R. Luthy and J.U. Bowie, 1997. VERIFY3D: Assessment of protein models with three-dimensional profiles. *Methods Enzymol.*, 277: 396-404.
37. Papadopoulos, F., M. Spinelli, S. Valente, L. Foroni, C. Orrico, F. Alviano and G. Pasquinelli, 2007. Common tasks in microscopic and ultrastructural image analysis using ImageJ. *Ultrastruct. Pathol.*, 31: 401-407.
38. Takashimizu, Y. and M. Iiyoshi, 2016. New parameter of roundness R . Circularity corrected by aspect ratio. *Progr. Earth Planetary Sci.*, Vol. 3. 10.1186/s40645-015-0078-x.
39. De Brevern, A.G., A. Bornot, P. Craveur, C. Etchebest and J.C. Gelly, 2012. PredyFlexy: Flexibility and local structure prediction from sequence. *Nucl. Acids Res.*, 40: W317-W322.
40. Bornot, A., C. Etchebest and A.G. de Brevern, 2011. Predicting protein flexibility through the prediction of local structures. *Proteins: Struct. Funct. Bioinform.*, 79: 839-852.
41. Yu, H., 1999. Extending the size limit of protein nuclear magnetic resonance. *Proc. Natl. Acad. Sci. USA.*, 96: 332-334.
42. Frueh, D.P., A.C. Goodrich, S.H. Mishra and S.R. Nichols, 2013. NMR methods for structural studies of large monomeric and multimeric proteins. *Curr. Opin. Struct. Biol.*, 23: 734-739.
43. Egli, M., 2010. Diffraction techniques in structural biology. *Curr. Protoc. Nucl. Acid Chem.*, 41: 7-35.
44. Cheng, Y., 2015. Single-particle cryo-EM at crystallographic resolution. *Cell*, 161: 450-457.
45. Devedjiev, Y.D., 2015. The role of flexibility and molecular shape in the crystallization of proteins by surface mutagenesis. *Acta Crystallogr. Sect. F: Struct. Biol. Commun.*, 71: 157-162.
46. Acharya, K.R. and M.D. Lloyd, 2005. The advantages and limitations of protein crystal structures. *Trends Pharmacol. Sci.*, 26: 10-14.
47. Carroni, M. and H.R. Saibil, 2016. Cryo electron microscopy to determine the structure of macromolecular complexes. *Methods*, 95: 78-85.
48. Floudas, C.A., H.K. Fung, S.R. McAllister, M. Monnigmann and R. Rajgaria, 2006. Advances in protein structure prediction and *de novo* protein design: A review. *Chem. Eng. Sci.*, 61: 966-988.
49. Brylinski, M., 2015. Is the growth rate of Protein Data Bank sufficient to solve the protein structure prediction problem using template-based modeling? *Bio-Algorithms Med-Syst.*, 11: 1-7.
50. Hryc, C.F., D.H. Chen, P.V. Afonine, J. Jakana and Z. Wang *et al.*, 2017. Accurate model annotation of a near-atomic resolution cryo-EM map. *Proc. Natl. Acad. Sci. USA.*, 114: 3103-3108.
51. Budiman, C., K. Bando, C. Angkawidjaja, Y. Koga, K. Takano and S. Kanaya, 2009. Engineering of monomeric FK506-binding protein 22 with peptidyl prolyl *cis-trans* isomerase. *FEBS J.*, 276: 4091-4101.
52. Budiman, C., C. Angkawidjaja, H. Motoike, Y. Koga, K. Takano and S. Kanaya, 2011. Crystal structure of N-domain of FKBP22 from *Shewanella* sp. SIB1: Dimer dissociation by disruption of Val-Leu knot. *Protein Sci.*, 20: 1755-1764.
53. Perticaroli, S., J.D. Nickels, G. Ehlers, H. O'Neill, Q. Zhang and A.P. Sokolov, 2013. Secondary structure and rigidity in model proteins. *Soft Matter*, 9: 9548-9556.
54. Perticaroli, S., J.D. Nickels, G. Ehlers and A.P. Sokolov, 2014. Rigidity, secondary structure and the universality of the Boson peak in proteins. *Biophys. J.*, 106: 2667-2674.